International Journal of Advanced Science and Research
ISSN: 2455-4227, Impact Factor: RJIF 5.12
www.allsciencejournal.com
Volume 2; Issue 4; July 2017; Page No. 42-49

Type II core/shell quantum dot structures and their optical properties

[*1] P Bichpuria, [2] AOudhia

[1] Department of Physics, Govt. V.Y.T. PG Autonomous College, Durg (C.G.), Raipur, Chhattisgarh, India
[2] Department of Physics, Govt. Nagarjun Autonomous College of Science, Raipur (C.G.), Raipur, Chhattisgarh, India

Abstract
Highly luminescent, and bio-compatible GSH capped CdTe quantum dots (GSH-CdTe QDs) were prepared through a facile microwave (MW) aided wet chemical method. The tunability of the emission wavelength of the as obtained nanostructure was achieved simply by varying the size of CdTe cores and thickness of the CdSe shell. In addition, an effective shell-coating route was developed for the synthesis of CdTe/CdSe core/shell (C/S) and CdTe/CdSe/ZnS core/shell/shell (C/S/S) nanostructures by adopting a low temperature route for shell deposition. The UV–vis optical absorption and Photoluminescence (PL) emission spectral study were employed to study the confinement of excitons within the C/S interface isolating them from the solution environment and consequently improving the stability of the nanostructure. Finally a mechanism of formation of type II C/S/S structure having better optical properties were proposed.

Keywords: quantum dots; capping; UV–vis optical absorption; photoluminescence (PL)

1. Introduction
The synthesis of colloidal semiconductor nanocrystals has received considerable attention since the last two decades due to their unique optical, optoelectronics, magnetic and electrical properties that are different from their bulk structure counterpart [1-2]. Semiconducting nanocrystals such as QDs have attracted more attention due to their unique optical properties such as narrow emission spectra, continuous absorption band, high chemical and photo-bleaching stability, surface functionality etc. leading to many potential applications including nanolasers, bio-labelling, and photovoltaic, etc. [3-4]. To date, many C/S hetero-structure QDs, having two different semiconductors incorporated into a single colloidal QDs have been reported [5]. Typically there are type I and type II C/S QDs with different carrier localizations, depending on the band structure offsets between the semiconducting core and the shell [6]. In type I QDs both the electrons and holes are confined in the core, in contrast, to type II QDs, where the electrons and holes are separated between the core and the shell, giving rise to a significant increase in the exciton lifetime, making them suitable for photovoltaics [7]. It has been reported that the CdTe/CdSe C/S QDs exhibit type II band alignment, facilitating charge separations upon absorption of visible light for solar cells [8]. Recently, the high-quality CdTe/CdSe hetero-structure QDs have been successfully synthesized via colloidal chemical routes [9-11]. However, these synthetic methods are performed at high temperatures consuming several hours.Further, the use of toxic organic solvents and production of agglomerated QDs with broad size distribution makes this process undesirable. So, it is advantageous to develop a facile method for a quicker synthesis of highly fluorescent type II C/S QDs in aqueous ion solution. Microwave-assisted synthesis employed in the present study, is known to be one of the most effective methods used for the synthesis of nanocrystals, advantageous mainly due to the reaction selectivity, high efficiency and greater controllability over the physical parameters of the product [12-13]. The green protocols developed in the present study uses a biological thiol and a tri-peptide GSH as stabilizer, which is found in abundance in cells and works both as a reducing and capping agent for the aqueous synthesis of CdTe/ CdSe QDs [14-16]. Moreover, all the operations could be performed in air, avoiding the need for inert atmosphere, due to the fact that K_2TeO_3, used by us as the source material for Te^{2-} ions, is air stable [17-22].
Further, the present study also investigates the possible tuning of the emission wavelengths of the as obtained C/S nanocrystals into the visible spectrum (530-690 nm) by changing the shell thickness and/or core size, through an identical procedure, which is highly desirable in case of QDs. The as synthesized C/S structures were further capped with an inorganic material with a higher energy gap, as a shell, to enhance the quantum yield and improve the spectrum purity. Herein, an additional ZnS shell was epitaxially over coated on the outer layer of the pre-prepared CdTe/CdSe C/S nanocrystals to get the CdTe/CdSe/ZnS C/S/S heterostructure.

2. Experimental
The protocol for aqueous synthesis of CdTe core, CdTe/CdSe C/S and CdTe/CdSe/ZnS C/S/S QDs, employes $CdCl_2$, $ZnCl_2$, K_2TeO_3, Na_2SeO_3, Na_2S, as Cd^{2+},Te^{2-},Se^{2-} and S sources respectively, along with $NaBH_4$ as the reducing agent.GSH works both as a reducing and capping agent for the aqueous synthesis of CdTe QDs.

2.1 Synthesis of CdTe core, C/S and C/S/S QDs
182 mg $CdCl_2.2.5H_2O$ was diluted with 40 ml of Toluene, 240 mg GSH, 10 mg Sodium citrate, 2ml of K_2TeO_3 and 20 mg of $NaBH_4$ were added into cadmium sol with constant stirring. Borax buffer solution was used to adjust the pH 10. The mixture was kept in ultra-sonicator for vigorous stirring. The as obtained mixture was kept in a MW oven for 1 min at 300W power. The mixture was cooled down to ~ 50°C. The as prepared CdTe solution was concentrated to ¼ th of the

original volume and was finally precipitated using 2-propanol and collected via centrifugation. CdTe QDs dispersion was prepared by re-dissolving this colloid precipitate in 3ml DD water. All the stock solution for CdSe and ZnS shell growth were prepared bydissolving corresponding precursor solutions in borax buffer solution in appropriate amounts.

A modified low temperature MW technique was adopted for the growth of CdTe/CdSe C/S nanocrystal. The obtained CdTe dispersion was transferred drop wise into the CdSe stock solution and was kept in a MW oven for 5 min at 300W power. The CdTe/CdSe C/S QDs were obtained from the mixture following the process described earlier in case of core synthesis and were re-dissolved in 3ml DD water to prepare C/S dispersion. Similarly for preparing CdTe/CdSe/ZnS C/S/S QDs (C/S/S), the as obtained CdTe/CdSe C/S solution was transferred drop wise into ZnS stock solution and the mixture was kept in a MW oven for 5 min at 200W power. The dispersion was prepared as described earlier.

2.2 Formulae Used

The formulae used for calculation of monolayers is as follows [24]:

(Volume of X monolayer of shell on a core of radius r)

$$V_{shell}(ML_X) = 4/3*\pi*[(r_{core}+X*d)^3 - r^3_{core}] \longrightarrow Eq^n (1)$$

(Number of shell monomers in X ML)

$$n_{shell}(ML_X) = [(\rho_{shell}*V_{shell}(ML_X)]/m_{shell} \longrightarrow Eq^n (2)$$

(Moles of shell needed to coat N_{core} moles of core QDs with X ML)

$$N_{shell} = n_{shell}(ML_X)*N_{core} \longrightarrow Eq^n \quad (3)$$

Where,

- $V_{shell}(ML_x)$ - Volume of the shell comparising X ML of shell,
- r_{core} - Radius of the core nanocrystals,
- d - Thickness of one ML of shell,
- $n_{shell}(ML_X)$ -Number of monomer units of shell per core nanocrystal,
- ρ_{shell} -Bulk density of shell in the wurtzite phase,
- m_{shell} -Mass of a shell monomer unit,
- N_{shell}- Number of moles of shell precursor needed to grow X ML of shell,
- N_{core}- Number of moles of core nanocrystal in the reaction volume.

The thickness of monolayers was controlled by ensuring that the volume of the precursor stock solution added in each cycle should not exceed the amount needed for a whole ML of the CdSe shell. This amount was calculated from the respective volumes of concentric spherical shells with 0.35 nm thickness for 1ML of CdSe. A high-quality CdTe/CdSe C/S QDs with the desired shell thickness and corresponding emission wavelength was thus obtained. For ensuring tunability of the PL emission, firstlythe CdSe shell of desired thickness were grown and after attaining the PL emission wavelength of the resulting CdTe/CdSe C/S QDs, a ZnS shell was consecutively epitaxially over coated around the outer layer of the CdTe/CdSe template to form the CdTe/CdSe/ZnS C/S/S QDs. In present study the CdTe core were obtained and various layers of CdSe shell were coated on it.The average sizes of the nearly dot-shaped C/S nanocrystals (2.77, 3.47, 4.17, and 4.87 nm) corresponding to QDs containing a one-, two-, three-, and four-ML CdSe shell and (6.11, 6.97nm) for a four –ML CdSe + one/two -ML ZnS shell, respectively was obtained theoretically, as per the formulae used. TEM studies were performed to check the legitimacy of the theoretical calculations employed here. The theoretical and TEM results are fairly compatible, validating our present method of calculation; the results are compiled in Table 1 in section 3.1.

For the present study, the average thickness of one monolayer of CdSe (d) is taken as 0.35 nm and that of one monolayer of ZnS (d) is taken as 0.31 nm, according to the obtained values of the lattice constants of the corresponding material [24].

3. Result and Discussion

Fig. 1 shows the schematic of the synthesized C/S/S structures, to explain the band gap engineering performed while formation. The CdTe/CdSe/ZnS C/S/S QDs synthesized in the present study has a typical type II C/S QD structure. The energy of the valence band of the CdTe core is independent of the thickness of the CdSe shell. Similarly, the energy of the conduction band of the CdSe shell is also independent of the size of the CdTe core. So both the core size and the thickness of the shell can influence the effective band gap of the C/S structure through quantum-confinement effects. As a result, tuning the PL emission range is feasible by the variation of both the core size and the shell thickness.

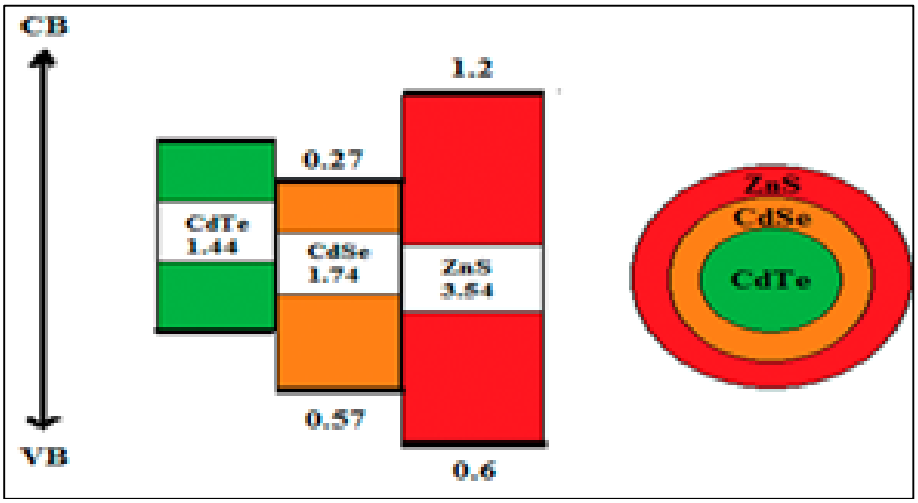

Fig 1: Schematic Diagram of energy bands (in eV) for CdTe, CdSe, and ZnS Interfaces [25] leading to a typical 'type II' QDs structure.

The QDs must suppress the non-radiative recombination on the surface and improve the confining potential. One of the ways to achieve this condition is by fully trapping the electrons and holes inside the core. This may also effectively suppress the non-radiative recombination of electrons and holes on the QDs surface due to the pressure of shell materials; hence the quantum yield could be increased [26]. The additional ZnS shell, with a substantially wide band gap, serves as a type-I heterojunction with the CdSe layer (the band offsets among CdTe, CdSe, and ZnS are shown in Fig. 1) [27], thus efficiently confining both electrons and holes within the CdTe/CdSe C/S structure and substantially enhancing the spatial indirect radiative recombination at the CdTe core and inner CdSe shell interface. By varying the size of CdTe cores and the thickness of the CdSe shell, the emission wavelength of the obtained nanostructure can span from 540 to 825 nm [28]. In addition, the passivation of the ZnS shell with a substantially wide band gap confines the excitons within the CdTe/CdSe C/S interface and isolates them from the solution environment and consequently improves the stability of the nanostructure, especially in aqueous media.

3.1 Morphology and structural studies

SEM and TEM studies were performed to study the morphologies and particle size distribution of the as prepared QDs.

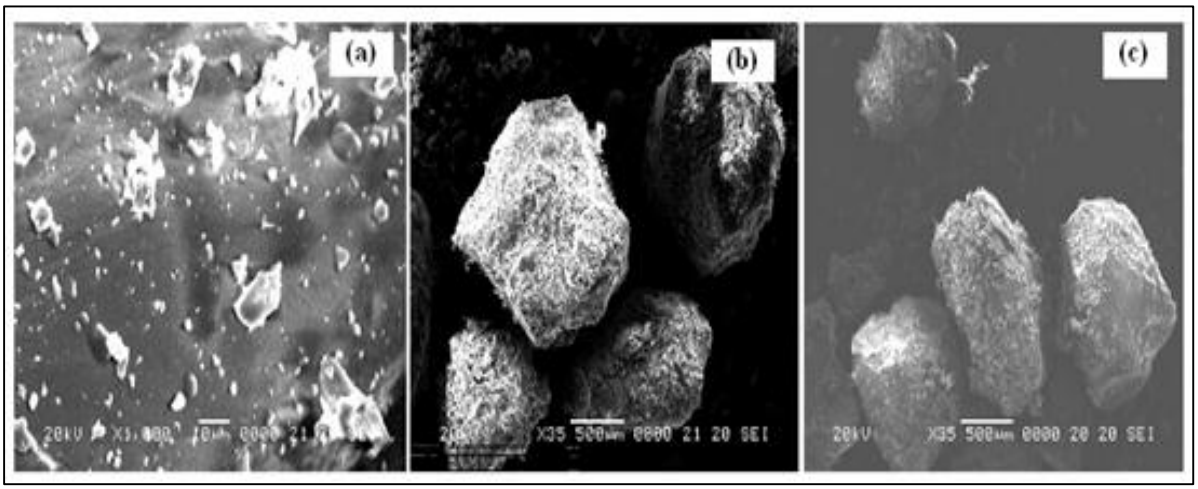

Fig 2: SEM micrographs of various QDs structures: (a) CdTe core QDs, (b) CdTe/CdSe C/S QDs and (c) CdTe/CdSe/ZnS C/S/S QDs.

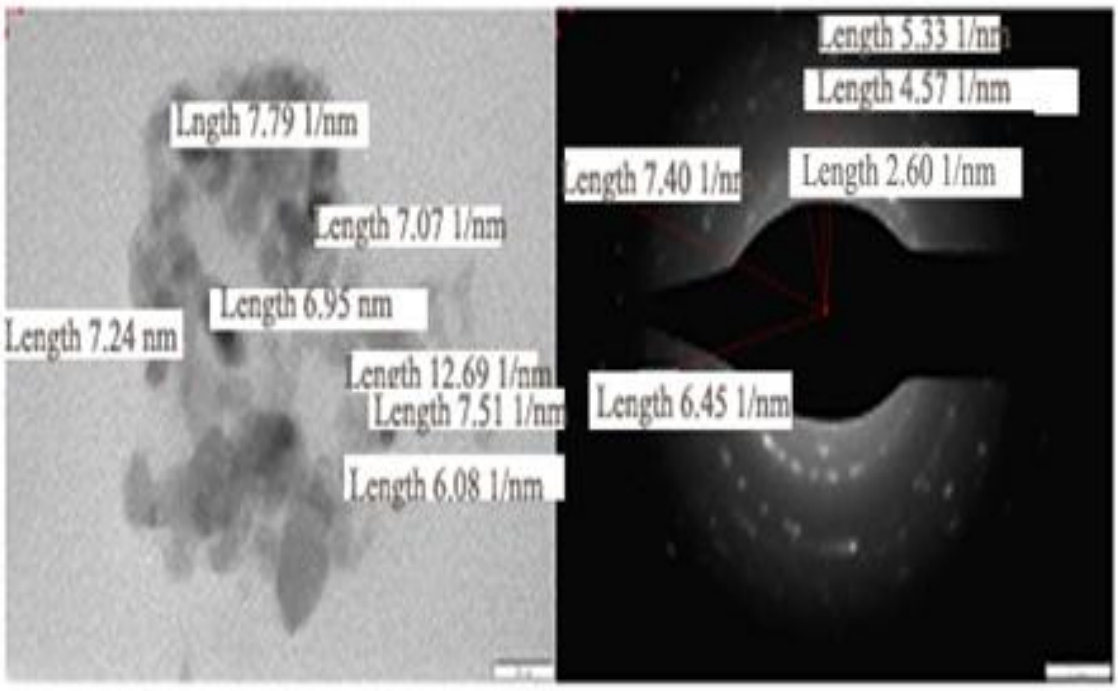

(a) **(b)**

Fig 3: TEM micrographs of C/S QDs: (a) An interface between CdTe core and CdTe/CdSe C/S in TEM and (b) Particle size dispersion 4.91 nm cross sectional study.

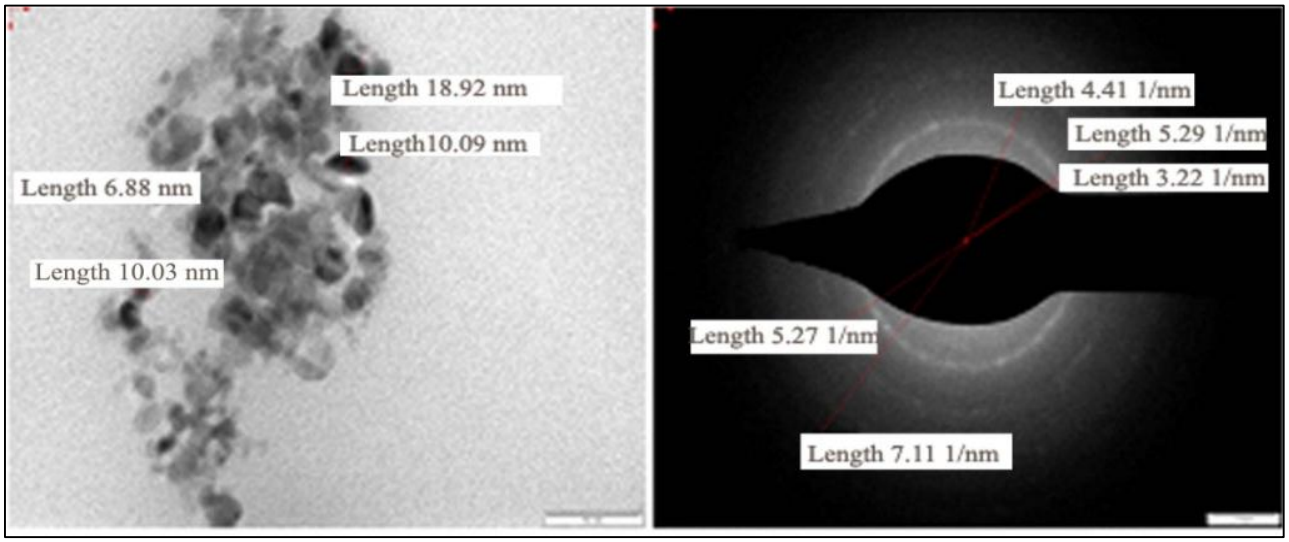

(a) **(b)**

Fig 4: TEM micrographs of C/S/S QDs: (a) No interface observed between CdTe/ CdSe C/S and ZnS shell in TEM and (b) Particle size dispersion 5.06 nm cross sectional study.

Fig. 2 shows SEM patterns at different magnification by SEM- JEOL JSM-5600. As observed in (Fig.2 (a)), a well dispersed CdTe core QDs structure was obtained through the microwave aided synthesis method. (Fig. 2 (b)) shows a high density of C/S structure, which grew bigger after the ZnS layer, was deposited on them, observed in (Fig. 2(c)). (Fig.3 and Fig.4) show the TEM images of C/S and C/S/S QDs were taken by PHILIPS TEM CM 200. TEM images further validates that the particle size dispersion is less, ranging between 2–10 nm. The TEM images show an interface between core CdTe (black) and shell CdSe (white), whereas no evidence of an interface between C/S and C/S/S is observed, which is consistent with a coherent epitaxial growth mechanism of ZnS shell, and demonstrates that the shell growth does not disturb the crystalline form of the C/S. Further, the TEM images observes increment in size resulting from the growth of the first (CdSe) and second (ZnS) shell, similarly, as observed in SEM and XRD studies. The sizes obtained by the Scherrer's formulae in the next section, also confirms the increase in size with shell formation. (Table.1) shows a comparative particle size distribution calculated theoretically and through TEM studies.

Table 1: The comparative Average particle size distribution calculated theoretically and through TEM studies

Types of QDs	Theoretically CalculatedParticle size (nm)	Average Particle size calculated through TEM(nm)
CdTe/CdSe C/S QDs(4ML)	4.87	4.91
CdTe/CdSe/ZnS C/S/S QDs(2ML)	6.97	5.06

Fig. 5 shows that the peaks obtained in the XRD studies were taken by XRD-Bruker/LynxEye1D-PSDX-ray generator using the Kα radiation of Cu at a wavelength of 1.542 Åmatched with the standard data for CdTe (JCPDS card no.65-1046), CdSe (JCPDS card no.00-019-0191) and ZnS (JCPDS card no.65-1691). The XRD results confirm the formation of C/S and C/S/S structures. The core shows a single peak corresponding to CdTe as observed in (Fig. 5 (a)). After the formation of CdSe shell, peaks corresponding to CdSe only is observed in (Fig. 5(b)).Similarly after the formation of C/S/S the XRD peaks corresponding to CdSe should not be observed in (Fig. 5(c)), but the peaks corresponding to only ZnS should be there. However since the specimen used for the XRD study includes the samples with only one monolayer of CdSe for C/S and one monolayer of ZnS for C/S/S structures, some peaks corresponding to the base materials also appear in the XRD pattern. The diffraction peaks are broadened due to the finite particle size. When the CdSe shell is overgrown around the cubic CdTe template, the general pattern of the cubic lattice is maintained in the C/S structures, but the diffraction peaks shift to larger angles consistent with the smaller lattice constant for CdSe compared with CdTe. With the further overgrowth of the ZnS shell around the outer layer of the CdTe/CdSe, the diffraction peak positions have no significant shift. In addition, the diffraction peaks narrow further with the over coating of shell materials. This narrowing indicates that the crystalline domain is larger for the C/S/S structure, providing direct evidence for epitaxial growth of the shell. XRD data is compiled in (Table. 2) for particle size calculations using Scherrer's formulae, strain and dislocation densities.

Table 2: Compiled XRD data for particle size calculations using Scherer's formulae

Sample	2θ	hkl	d (Å)	FWHM(Degree)	Crystallite SizeD (nm)	Strain($lin^{-2}m^{-4}$)	DislocationDensity (lin/m^2)
CdTe QDs	27.67	(102)h	3.222E-10	0.87574	9.13	0.015513	1.2E+16
CdTe/CdSe C/S QDs	28.25	(102)h	3.158E-10	0.0972	82.3	0.001685	1.48E+14
CdTe/CdSe/ZnS C/S/S QDs	32.17	(200)c	2.782E-10	0.03572	226	0.000541	1.96E+13

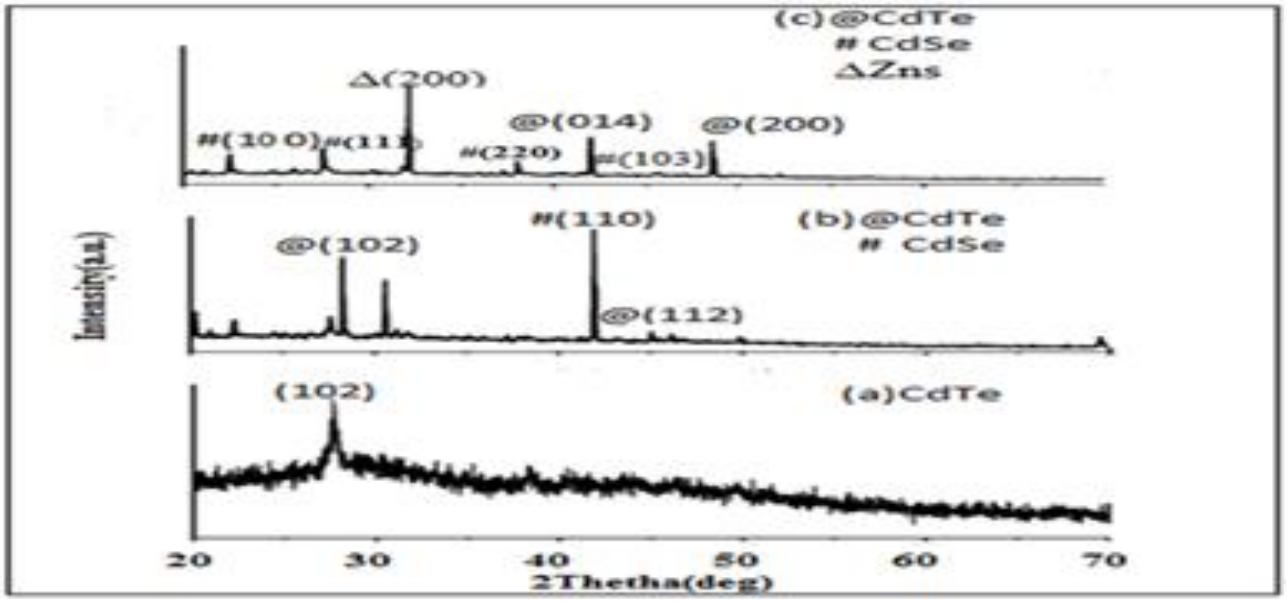

Fig 5: XRD pattern of various QDs structures:(a) GSH-CdTe core QDs, (b) GSH-CdTe/CdSe C/S QDs and(c) GSH-CdTe/CdSe/ZnS C/S/S QDs showing structural changes with the growth of various shell layers.

3.2 Optical Studies

Fig. 6 shows the optical absorption spectra of core, C/S and C/S/S QDs. The optical absorption was investigated using UV–Vis spectrophotometer (Varian Carry 50 BIO). With the increase of the CdSe shell thickness, a systematic red-shift was observed the absorption peaks of the resulting CdTe/CdSe C/S nanocrystals. On analysing the absorption spectra with the overgrowth of shell material CdSe around the CdTe cores, it is found that, on one hand, the spectral profiles red-shift and, on the other hand, the distinctive absorption peaks of the initial GSH-CdTe core QDs (the hump observed at ~530nm in the optical absorption curves in (Fig. 6(a)) are eroded gradually; the excitonic absorption peak broadens; and finally evolves into a featureless absorption tail when the shell thickness is two MLs. The observance of this featureless absorption tail in the absorption spectrum can be attributed to the spatial separation of the charge carrier in type-II C/S QDs and because of this, type-II C/S QDs effectively behave as indirect semiconductors near the band edges [5, 6]. Further, the relative absorbance of CdTe/CdSe C/S QDs shows a notable increase over the cores in the short wavelength region. This can be attributed to the higher effective density of states due to their larger size, however, they have relatively little absorbance near the band edge because of the weaker oscillator strength resulting from the decreased wave function overlap due to the spatial separation of the charge carriers [28]. For C/S/S structures the optical absorption increases with increasing thickness of ZnS layers, as observed in (Fig. 6(b)).

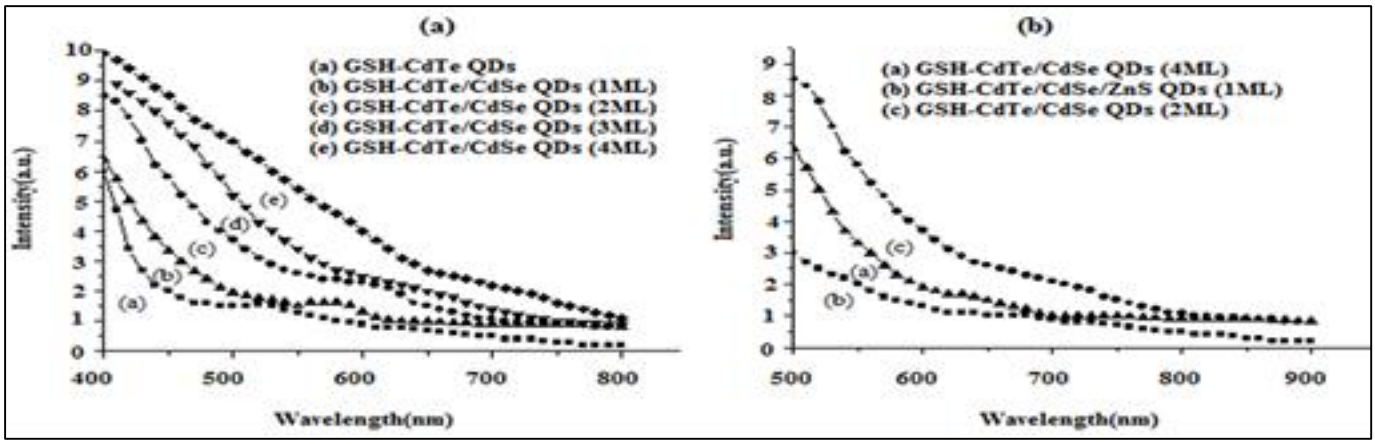

Fig 6: Optical absorption spectra of various QDs structures: (a) CdTe/CdSe C/S with varying shell thickness with 1ML, 2ML,3ML and 4ML respectively and (b) CdTe/CdSe/ZnS C/S/S QDs with 4ML CdSe shell + 1and 2 ML ZnS shell thickness.

The evolution of absorption spectra clearly demonstrates a progressive reduction of the electron-hole function overlap and the formation of the indirect exciton as the dimension of the CdSe shell increased, ultimately leading to characteristic type-II behaviour. The gradual evolution of semiconductor heterostructures from type-I toward a type-II optical behaviour has also been reported in CdTe/CdSe[29-35] and CdS/ZnSe systems [36, 37]. Figure 7 shows the effect of varying shell thickness on the PL emission of obtained QDs.PL spectra were measured using PL- LS 45 Perkin Elmer Luminescence Spectrophotometer. The emission of type-II C/S QDs originates from the radiative recombination of

electron hole pairs across the C/S interface. This can explain why the emission from the CdTe/CdSe C/S is observed at wavelengths longer than the band gap emission of either CdTe or CdSe with the same size. with the increase of the CdSe shell thickness to one, two, three, and four MLs, the corresponding PL peaks shift to λ=560, 600, 640 and 690 nm, respectively, from the original λ = 530 nm for the CdTe cores.

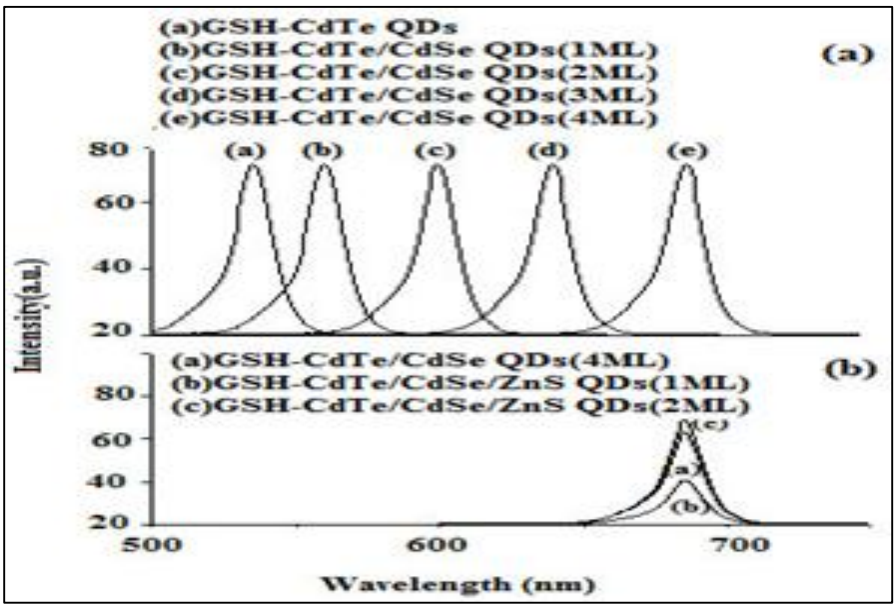

Fig 7: PL spectra of various QDs structures with varying shell thickness: (a)The red shift in the PL peaks of CdTe, CdTe/CdSe, CdTe/CdSe/ZnS QDs with varying shell CdSe thickness and (b) The enhancement of PL intensity with the overgrowth of ZnS shell structure.

The PL emission of CdTe/CdSe C/S QDs should be attributed to an excitonic transition involving the relaxed electron (mainly localized in the conduction band of the CdSe shell) and hole states (mainly localized at the valence band of the CdTe core), which is illustrated in (Fig.7).It has been proven that the surface passivation of nanocrystals with a suitable inorganic material having a higher bandgap is the key to improving PL efficiency and the stability of nanocrystals [37].When one ML of CdSe is grown around the CdTe cores no substantial change in the PL emission spectra was observed, although a slight red shift of the emission wavelength was observed. The radiative recombination is quenched because of the presence of some imperfections like traps on the crystal. These traps are Cd or Te atoms with dandling bonds, which can attract electron and holes, respectively, acting as mid gap states. In the case of an electron, which is declining from the conduction band, it can be captured by a trap and then relax to the valence band without emitting. The results show that the low temperature protocol adopted for synthesis of ZnS shell effectively caps the C/S, controls the particle size distribution and decreases the surface defects resulting in a remarkable enhancement in PL intensity [38]. It can be observed that the low temperature synthesis of ZnS shell was favourable for the epitaxial growth of a ZnS shell with a high degree of crystallinity (see XRD fig 5(c)).The C/S/S structure show increase in PL intensity with increasing ML of ZnS, as can be also observed by PL peak in (Fig. 7(b). The additional ZnS shell, with a substantially wide band gap, serves as a type-I heterojunction with the CdSe layer [27], thus efficiently confining both electrons and holes within the CdTe/CdSe structure and substantially enhancing the spatial indirect radiative recombination at the CdTe core and inner CdSe shell interface, which is evident from the sharp XRD peaks (Fig. 5(b)).

4. Conclusions

This study presents a quick and cost effective method of synthesis of highly luminescent QDs with bare core, C/S and C/S/S structures using microwave aided wet chemical synthesis method. The GSH capped biocompatible and stable QDs were obtained without compromising their optical properties. The TEM study validates the formation of C/S and C/S/S structure with small particle size dispersion. The optical studies confirm the formation of type II QD structure. The optical properties of the QDs were tuned within a given visible range by varying the shell thickness. The type II QDs thus formed can enhance the efficiency of QDs solar cells by increasing the charge separation.

5. Acknowledgements

The authors gratefully acknowledge the facilities provided by the following colleagues Dr.D.M. Phase Scientist-G, and V. K. Ahire for SEM and Dr.Mukul Gupta- Scientist-E for XRD, UGC-DAE-CSR, Indore Centre, Dr. Ravi Sharma, Asst. Prof. Dept. of Physics. Arts and Commerce Girls College, Devendra Nagar, Raipur (C.G.) for PL studies, Prof. D. P. Bisen, SOS Physics, Pt. RSSU, Raipur (C.G.) for UV–Vis optical absorption studies, and Asst.Prof. Rajesh kumar, BIT, Durg for XRD result analysis.

6. References

1. Alivisatos AP. Semiconductor clusters, nanocrystals & quantum dots, Sci.1996; 271:933-937.
2. Lee S, Dobrowolska M, Furdyna JK. CdSe self-assembled quantum dots grown on ZnMnSe diluted magnetic semiconductors with different Mn concentration, J. Crystal Growth. 2006; 292:311-314.
3. Bruchez M, Moronne M, Gin P, Weiss S, Alivisatos AP. Semiconductor Nano crystals as fluorescent biological

labels, Sci. 1998; 281:2013-2016.
4. Tsutsui T. Applied physics - a light-emitting sandwich filling, Natr. 2002; 420:752-755.
5. Kim S, Fisher B, Eisler HJ, Bawendi M. Type-II quantum dots: CdTe/CdSe(core/shell) and CdSe/ZnTe (core/shell) heterostructures, J. Am. Chem. Soc. 2003;125:11466-11467.
6. Balet LP, Ivanov SA, Piryatinski A, Achermann M,KlimovVI. Inverted core/shell nanocrystals continuously tunable between type-I and type-II localization regimes, Nano Lett. 2004; 4:1485-1488.
7. Lo SS, Mirkovic T, Chuang CH, Burda C, Scholes GD. Emergent propertiesresulting from type-II band alignment in semiconductor nanoheterostructures, Adv. Mater. 2011; 23:180-197.
8. Zhong H, Zhou Y, Yang Y, Yang C, Li Y. Synthesis of type II CdTe-CdSenanocrystalheterostructured multiple-branched rods and their photovoltaic applications, J. Phys. Chem.C. 2007; 111:6538-6543.
9. Xia YS, Zhu CQ. Aqueous synthesis of type-II core/shell CdTe/CdSequantum dots for near-infrared fluorescent sensing of copper (II), Analyst. 2008; 133:928-932.
10. Zeng RS, Zhang TT, Liu JC, Hu S, Wan Q, Liu XM, *et al*. Aqueous synthesis of type-II CdTe/CdSe core-shell quantum dots for fluorescent probe labelingtumor cells, Nanotechnol. 2009; 20:095-102.
11. Zhang Y, Li Y, Yan XP. Aqueous layer-by-layer epitaxy of type-II CdTe/CdSe quantum dots with near-infrared fluorescence for bioimaging Applications, Small. 2009; 5:185-189.
12. Gerbec JA, Magana D, Washington A, Strouse GF. Microwave-enhanced Dallinger D, Kappe CO. Microwave-assisted synthesis in water as solvent, Chem. Rev. 2007; 107:2563-2591.
13. Zhu MQ, Gu Z, Fan JB, Xu XB, Cui J, Liu JH, *et al*. Microwave-mediated nonaqueous synthesis of quantum dots at moderate temperature, Langmuir. 2009; 25:10189-10194.
14. Schafer FQ, Buettner GR. Redox environment of the cell as viewed through theredox state of the glutathione disulfide/glutathione couple, Free Radic. Biol. Med. 2001; 30:1191-1212.
15. Tian J, Liu R, Zhao Y, Xu Q, Zhao S. Controllable synthesis and cell-imagingstudies on CdTe quantum dots together capped by glutathione and thioglycolic acid, J. Colloid. Interface Sci. 2009; 336:504-509.
16. Zheng Y, Gao S, Ying J. Synthesis and cell-imaging applications of glutathione capped CdTe quantum dots, Adv. Mater. 2007; 19:376-380.
17. CalderónI L, Arenas FA, Pérez JM, Fuentes DE, Araya MA, *et al*. Catalases are NAD(P)H-dependent telluritereductases, PLoS ONE. 2006; 1:70.
18. Pérez JM, Pradenas GA, Navarro CA, Henríquez DR, Pichuantes SE, *et al*. Geobacillusstearothermophilus LV cadA gene mediates resistance to cadmium, lead and zinc in zntA mutants of Salmonella entericaserovar Typhimurium, Biol. Res. 2006; 39:661-668.
19. Pérez JM, Calderón IL, Arenas FA, Fuentes DE, Pradenas GA, *et al*. Bacterialtoxicity of potassium tellurite: unveiling an ancient enigma, PLoS ONE. 2007; 2:211.
20. Chasteen TG, Fuentes DE, Tantaleán JC, Vásquez CC. Tellurite: history, oxidative stress, and molecular mechanisms of resistance, FEMS Microbiol. Rev. 2009; 33:820-832.
21. Helbig K, Bleuel C, Krauss GJ, Nies DH. Glutathione and transition-metalhomeostasis in Escherichia coli, J. Bacteriol. 2008; 190:5431-5438.
22. Turner RJ, Weiner JH, Taylor DE. Tellurite-mediated thiol oxidation in Escherichia coli, Microbiol. 1999; 145:2549-2557.
23. Reiss Peter, Myriam Protière, Liang Li. Core/Shell Semiconductor Nanocrystals, Small. 2009; 5:154-168.
24. Dabbousi, Bashir O. Fabrication and Characterization of Hybrid Organic/Inorganic Electroluminescent Devices Based on Cadmium Selenide Nanocrystallites (Quantum Dots)" Ph.D thesis, Massachusetts Institute of Technology, 1997.
25. Wei SH, Zunger A. Calculated natural band offsets of all II–VI and III–V semiconductors: Chemical trends and the role of cation d orbitals, Appl. Phys. Lett. 1998; 72:2011-2013.
26. Steckel JS, Zimmer JP, Coe-Sullivan SN, Stott E, Bulovic V, Bawendi MG. Blue luminescence from (CdS)ZnS core-shell nanocrystals, Angew. Chem. Int. Ed. 2004; 43:2154-2158.
27. Wenjin Zhang, Guanjiao Chen, Jian Wang, Bang-Ce Ye, Xinhua Zhong. Design and Synthesis of Highly Luminescent Near-Infrared-Emitting Water-Soluble CdTe/CdSe/ZnS Core/Shell/Shell Quantum Dots, Inorg. Chem. 2009; 48:9723-9731.
28. Laheld UEH, Pedersen FB, Hemmer PC. Excitons in type II quantum dots: Finite offsets, Phys. Rev. B. 1995; 52:2697.
29. Kim S, Fisher B, Eisler HJ, Bawendi MG. Type-II Quantum Dots: CdTe/CdSe (Core/Shell) and CdSe/ZnTe(Core/Shell) Heterostructures. J. Am. Chem. Soc. 2003; 125:11466-11467.
30. Chin PTK, De Mello Donega C, Van Bavel SS, Meskers SCJ, Janssen RAJ. Highly luminescent CdTe/CdSe colloidal heteronanocrystals with temperature- dependent emission color, J. Am. Chem. Soc. 2007; 129:14880-14886.
31. Yu K, Zaman B, Romanova S, Wang DS, Ripmeester JA. Sequential synthesis of type II colloidal CdTe/CdSe core-shell nanocrystals,Small.2005;1:332-8.
32. Milliron DJ, Hughes SM, Cui Y, Manna L, Li JL, Wang W, *et al*. Colloidal nanocrystalheterostructures with linear and branched topology, Natr. 2004; 430:190-5.
33. Halpert JE, Porter VJ, Zimmer JP, Bawendi MG. Synthesis of CdSe/CdTeNanobarbells. J. Am. Chem. Soc. 2006; 128:12590-12591.
34. Li JJ, Tsay JM, Michalet X, Weiss S. Wavefunction engineering: From quantum wells to near-infrared type-II colloidal quantum dots synthesized by layer-by-layer colloidal epitaxy. Chem. Phys. 2005; 318:82-90.
35. Seo H, Kim SW. In Situ Synthesis of CdTe/CdSe Core−Shell Quantum Dots. Chem. Mater. 2007; 19:2715-2717.
36. Ivanov SA, Piryatinski A, Nanda J, Tretiak S, Zavadil KR, Wallace WO, *et al*. Type-II core/shell CdS/ZnSenanocrystals: synthesis, electronic structures, and spectroscopic properties. J. Am. Chem. Soc. 2007; 129:11708-11719.

37. Fang Z, ZGu Z, Zhu W, Zhong X. Design and Synthesis of High-Quality CdS/ZnSeType-II Core/Shell Nanocrystals. J. Nanosci. Nanotechnol. 2009; 9(5):880-886.
38. Qu L, Peng XG. Control of Photoluminescence Properties of CdSeNanocrystals in Growth. J. Am. Chem. Soc. 2002; 124:2049-2055.